Nonlinear Induced Disturbance Rejection in Inertial Stabilization Systems

Bo Li, David Hullender, and Mike DiRenzo

***Abstract*—A frequent problem in inertial stabilization control systems is the rejection of disturbances associated with moving components. Very often such disturbances are nonlinear and time varying. A prime example is the relative motion of components within a gimbal; in this case, nonlinear bearing friction induces a destabilizing torque from base motion to the component being stabilized. This paper presents an linear quadratic Gaussian (LQG) algorithm, based on a simple first-order linear stochastic differential equation, for estimating and compensating in real time a particular class of disturbances that can be modeled as a plus or minus unknown slowly changing random value such as is characterized by nonlinear Coulomb friction. Results of computer simulations testing the control algorithm are presented along with actual measurements from a laboratory brassboard system. The results reveal a noteworthy improvement in disturbance rejection as compared with a conventional proportional integral (PI) controller with notch filters.**

***Index Terms*—Bearing friction, Coulomb friction, gimbal, LQG control, stabilization.**

I. Introduction

A single-axis mass-stabilized gimbal rate control system consists of a gyro which provides feedback measurement of the inertial angular rate of the object being stabilized [1]. In general, the actual rate $\dot{\theta}$ is compared with the input command rate $\dot{\theta}_c$ to determine the rate error. This angular rate error drives a digital controller that drives a torque motor that induces a correction torque to the gimbal for purposes of stabilization. The objective of being able to reduce stabilization errors is a never ending task as performance specifications on tracking and optical sighting systems continue to increase.

The block diagram of an actual laboratory brassboard gimbal rate control system [2], [3] is shown in Fig. 1. Note that the rate error is corrupted by gyro noise, $v(t)$, and by the gyro structural dynamics. Also, note that the gimbal structural dynamics have been approximated by the rigid body mode plus one structural bending mode. As shown in Fig. 1, the relative motion, $\dot{\theta} - \dot{\theta}_B$, between the base of the gimbal and the component being stabilized produces a destabilizing torque T_f associated with bearing friction, which must be rejected by the digitally controlled torque motor which has gain K_T.

This paper presents and evaluates a real time estimation and control algorithm for disturbance rejection in this laboratory brassboard stabilization system. A first-order linear stochastic differential equation is incorporated to estimate gimbal bearing friction. This linear equation in no way represents an accurate model for nonlinear gimbal bearing friction [4]–[7]. However, it is of a form that is compatible with the Kalman filter equations. As will be demonstrated, this stochastic differential equation characterizes a slowly changing random process that accurately identifies the effects of the actual nonlinear friction on the system. Consequently, friction identification and effective compensation are achieved. The algorithm is tested using numerical simulation techniques and then tested in the laboratory using the actual brassboard hardware with a TMS 320 microprocessor operating in real time.

Since it was relatively straightforward to measure the gimbal structural dynamics on this laboratory brassboard system, this paper presents results based on the assumption that these structural resonance characteristics are known and do not change. As will be demonstrated in this paper for a case of such plant dynamics being known, the controller rejects the nonlinear friction disturbance quite effectively and significantly better than a conventional PI controller with notch filters originally designed by control engineers specifically for this brassboard system.

The formulation of an algorithm to adapt or self-tune these estimation and control equations for cases where the plant dynamics are either unknown or changing is the subject of a follow-up paper [8].

II. Friction Estimator

Friction between moving components not only varies with time but is nonlinear [4]–[7]. Such undesirable forces and torque result from the relative motion of two components that have not been perfectly isolated from each other. For gimbals used in stabilization and tracking systems, this relative motion usually corresponds to random base motion relative to the gimbal mounted component that one is trying to isolate and keep from moving. This component might be a robot arm, the barrel of a weapon, an optical sighting system, etc. [1]. This concept is illustrated in Fig. 2(a) and (b).

As shown in Fig. 2(b), the disturbance torque associated with this simple representation of bearing friction is either $+T_o$ or $-T_o$ depending on the sign of $\Delta\dot{\theta}$. Obviously, there is the possibility of viscous effects, zero relative velocity stiction effects, and hysteresis which may be present but not shown here [4]–[7]. This simple representation of $\pm T_o$ was used in the numerical simulation portion of this study to determine if the theoretical performance improvement with such a simple friction model justified an actual real-time implementation of the algorithm on the brassboard system.

Manuscript received May 30, 1996. Recommended by Associate Editor, R. Ravi. This work was supported by a grant from Texas Instruments, Inc.

B. Li is with Ericsson, Inc., Richardson, TX 75081 USA.

D. Hullender is with the Department of Mechanical Engineering, The University of Texas at Arlington, Arlington, TX 76019 USA.

M. DiRenzo is with Texas Instruments, Inc., Dallas, TX 75235 USA.

Publisher Item Identifier S 1063-6536(98)02999-6.

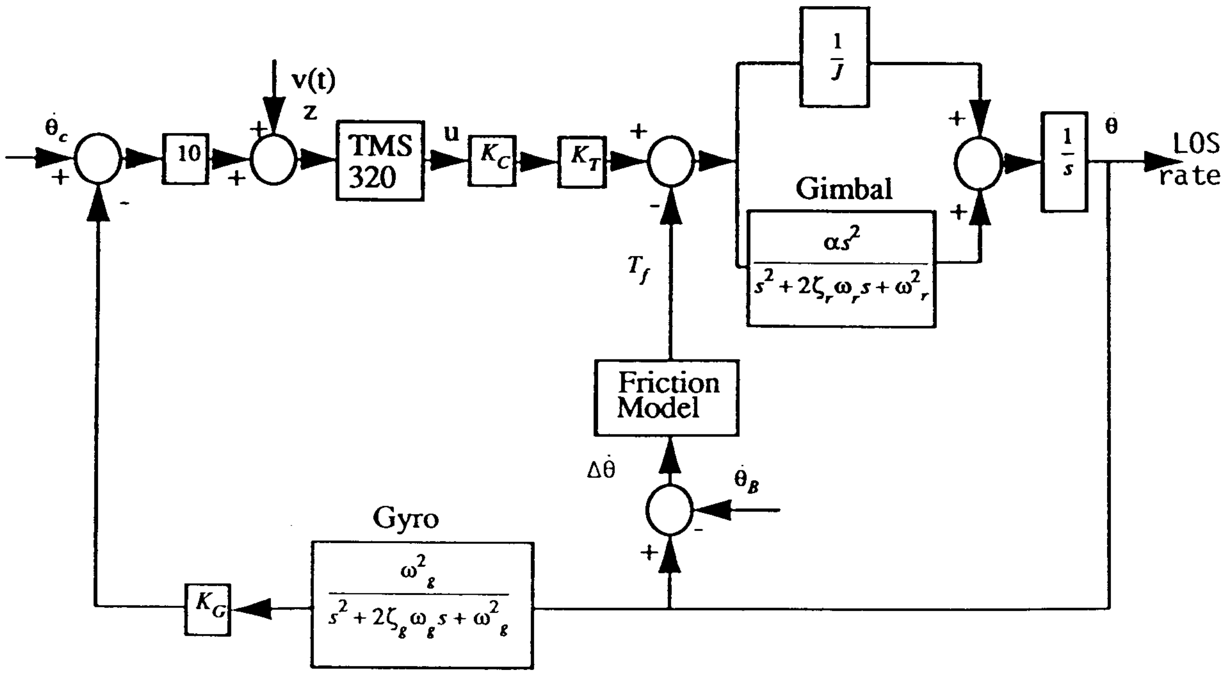

Fig. 1. Block diagram of the brassboard gimbal system.

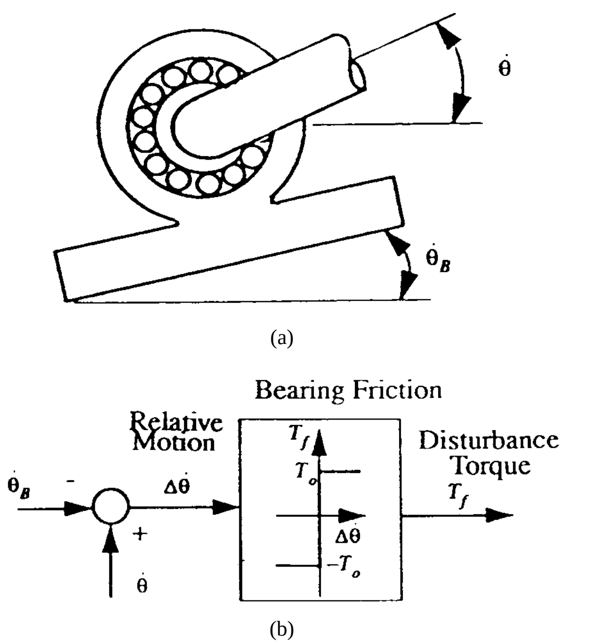

Fig. 2. (a) Schematic of a gimbal and (b) block diagram for gimbal friction.

If we assume that the switching of the friction from plus to minus is at a relatively low frequency compared to the sampling frequency, then it is possible to approximate the model for the friction as being exponentially correlated with time constant τ that is significantly greater than the inverse of the sample rate [2], [3], i.e.,

$$\frac{dT_f}{dt} = -\frac{1}{\tau}T_f + w \tag{1}$$

where w is white noise. This simple first-order equation allows for the use of the Kalman filter equations for estimating the friction.

III. Plant Equations and Estimation Algorithm

Referring to Fig. 1, the plant equations can be expressed as

$$\dot{X} = AX + Bu + Dw \tag{2}$$

$$z = CX + 10\dot{\theta}_c + v \tag{3}$$

where u is the feedback control which will be used to compensate for the system dynamics as well as for the friction; $\dot{\theta}_c$ is a reference input; z is the measurement; and X is the state vector. The first three state variables represent the gimbal modes, the fourth- and fifth-state variables represent the gyro dynamics, and the sixth-state variable is the friction T_f. Thus, the matrices for (2) and (3) can be shown to be

$$A = \begin{bmatrix} 0 & 1 & 0 & 0 & 0 & -\left(\alpha + \frac{1}{J}\right) \\ 0 & -2\zeta_r\omega_r & 1 & 0 & 0 & 2\zeta_r\omega_r\alpha \\ 0 & -\omega_r^2 & 0 & 0 & 0 & -\omega_r^2\alpha \\ 0 & 0 & 0 & -2\zeta_g\omega_g & 1 & 0 \\ \omega_g^2 & 0 & 0 & -\omega_g^2 & 0 & 0 \\ 0 & 0 & 0 & 0 & 0 & -1/\tau \end{bmatrix} \tag{4}$$

$$B = K_cK_T \begin{bmatrix} \left(\alpha + \frac{1}{J}\right) \\ -2\zeta_r\omega_r\alpha \\ \omega_r^2\alpha \\ 0 \\ 0 \\ 0 \end{bmatrix} \tag{5}$$

$$D = \begin{bmatrix} 0 \\ 0 \\ 0 \\ 0 \\ 0 \\ 1 \end{bmatrix} \tag{6}$$

$$C = [0 \quad 0 \quad 0 \quad -10K_G \quad 0 \quad 0]. \tag{7}$$

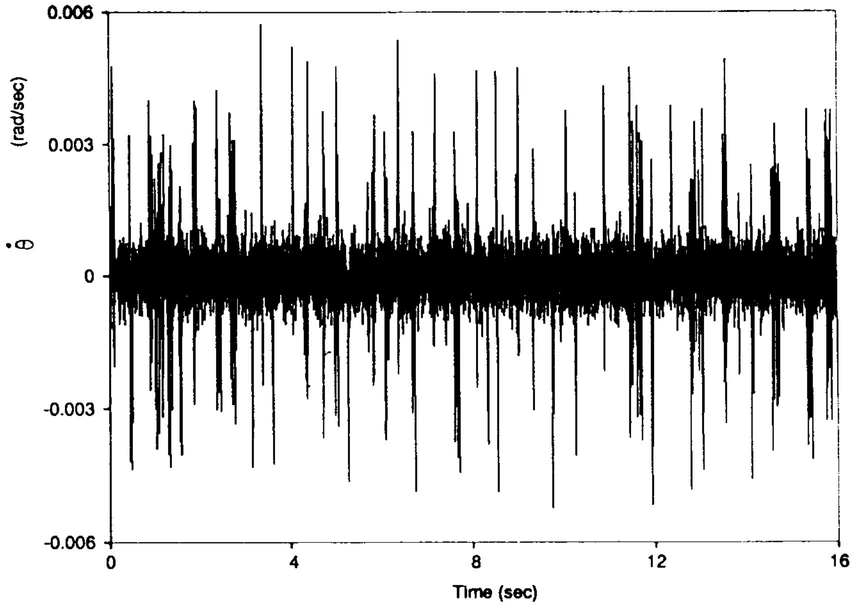

Fig. 3. Time history of LOS rate.

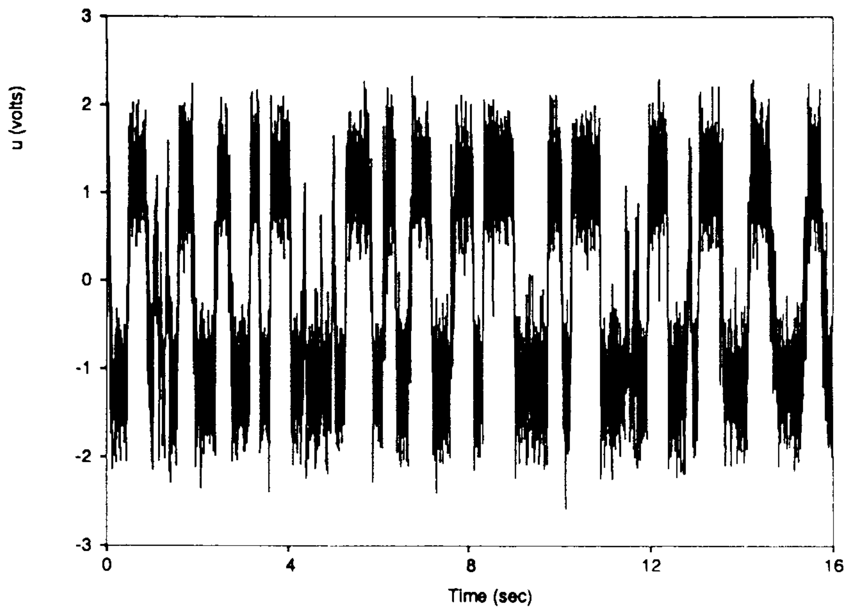

Fig. 4. Time history of control u.

A sensitivity study revealed that there was little change in performance once τ became much greater than the inverse of the sampling rate. Since it was desired to estimate an unknown random constant that occurs for a relatively long duration of time, a value of ∞ was used for τ to simplify the model.

Discretizing the plant and Kalman filter equations based on u, v, and w being piece-wise constant during a sample period, gives

$$X_{k+1} = A_d X_k + B_d u_k + D_d w_k \tag{8}$$

$$z_k = C X_k + 10\dot{\theta}_{ck} + v_k \tag{9}$$

$$\hat{X}_{k+1} = \overline{X}_k + K(z_k - C\overline{X}_k - 10\dot{\theta}_{ck}) \tag{10}$$

$$\overline{X}_k = A_d \hat{X}_k + B_d u_k \tag{11}$$

where $w_k \sim (0, Q/T)$; $v_k \sim (0, R/T)$.

IV. Control Algorithm

A linear quadratic Gaussian (LQG) control algorithm for the following general quadratic performance index has been used to calculate the feedback control gains

$$\mathrm{PI} = \tfrac{1}{2} \sum_{k=0}^{N} [X_k^T S_N X_k + R_u u_k^2] \tag{12}$$

where S_N is a weighting matrix and R_u is weighting constant.

If the parameters of the system are assumed constant and the measurement noise and base motion assumed to be stationary, then it is possible to use the steady-state solution [9], S, for the matrix Riccati equation to compute the control gains

$$\begin{aligned} G &= [g_1 \quad g_2 \quad g_3 \quad g_4 \quad g_5 \quad g_6] \\ &= [B_d^T S B_d + R_u]^{-1}(B_d^T S A_d). \end{aligned} \tag{13}$$

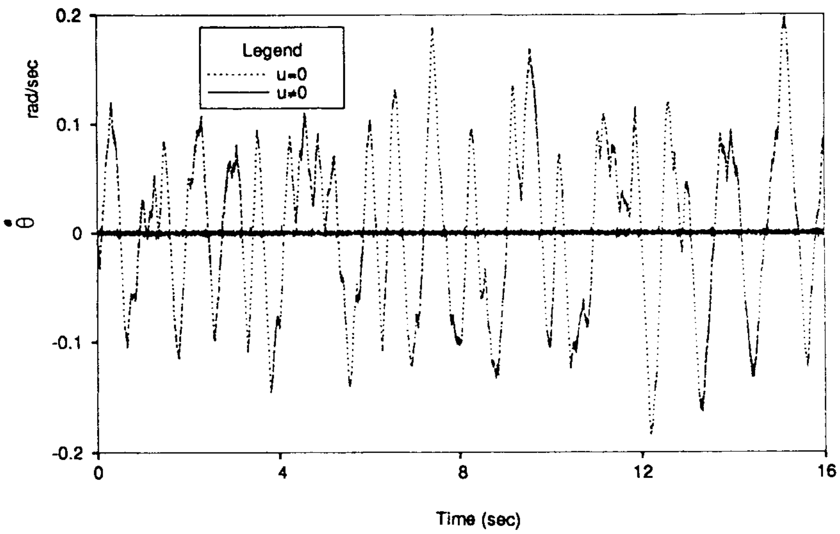

Fig. 5. Comparison of LOS rate when control is and is not applied.

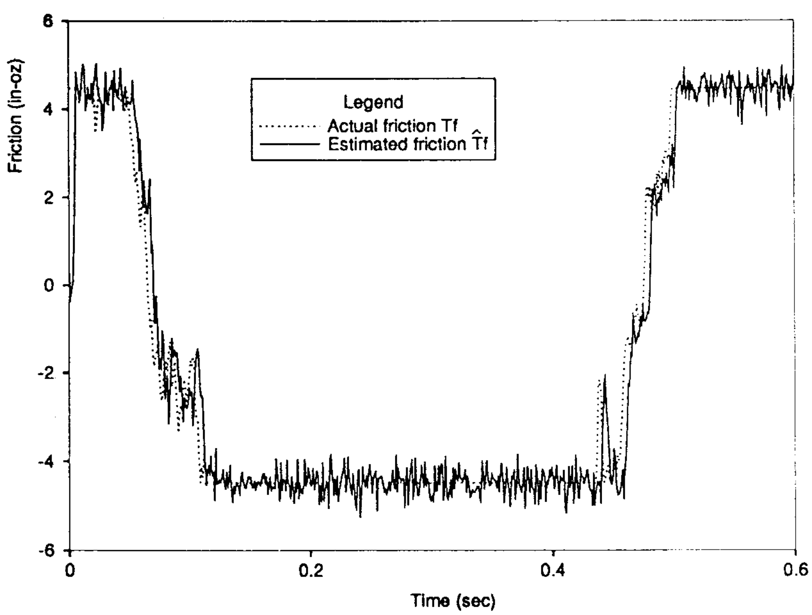

Fig. 6. Comparison of actual friction with the estimate of friction.

Our objective is to obtain a controller that will minimize following performance index:

$$\mathrm{PI} = \frac{1}{2}\sum_{k=0}^{N}\left[\left(\dot{\theta}_k - \frac{\dot{\theta}_{ck}}{K_G}\right)^2 + R_u u_k^2\right]. \tag{14}$$

Thus, the control u is of the form

$$u_k = -GX_k - g_c\dot{\theta}_{ck}. \tag{15}$$

It can be shown that the following state variable feedback is required:

$$u_k = -g_1\hat{x}_{1k} - g_2\hat{x}_{2k} - g_3\hat{x}_{3k} + \frac{1}{K_cK_T}\hat{T}_f + \frac{g_1}{K_G}\dot{\theta}_{ck}. \tag{16}$$

$S_N$is selected when $\dot{\theta}_{ck}$in (14) is zero. It is important to note that state variables $\hat{x}_4$ and $\hat{x}_5$ have not been included in the control algorithm. This is because the gyro dynamics have no bearing on the control gains even though they do affect the measurement z and, consequently, the calculation of estimator gains.

Examination of (16) reveals that the next to the last term will cancel T_f (see Fig. 1) if the estimate of T_f, $\hat{T}_f$, is fairly accurate. Also, the last term must have the same gain as that for $\hat{x}_1$ (except divided by K_G and opposite in sign); otherwise $\dot{\theta}$ will not equal the command rate $\dot{\theta}_c$, in steady state.

V. Computer Simulation Analysis

To demonstrate the potential levels of improvement in stabilization associated with these estimation and control algorithms, numerous computer simulations of the system have been conducted. For the purpose of simulation, the measurement noise $v(t)$ was assumed to be a zero mean, band-limited

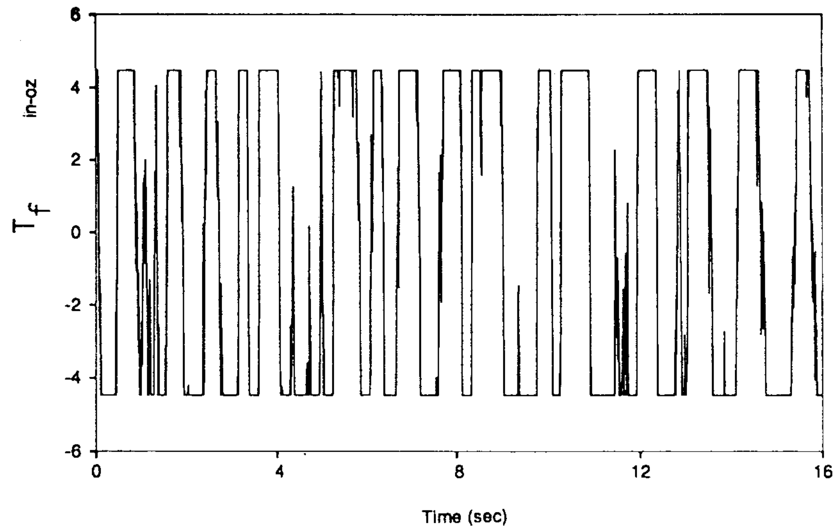

Fig. 7. Time history of actual friction.

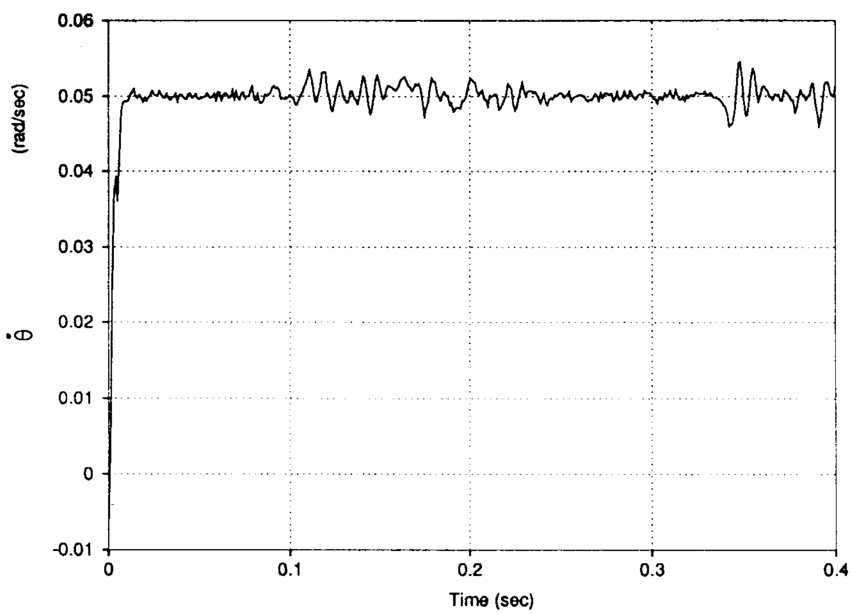

Fig. 8. LOS rate response for constant input command 0.05 rad/s.

white noise with a two-sided spectral density level of $R = 5 \times 10^7\,\mathrm{V}^2/\mathrm{Hz}$. The base motion, $\dot{\theta}_B(t)$, was generated by processing zero mean, band-limited white noise $w_b(t)$ with a two-sided spectral density of 0.5 through a shaping filter with the following transfer function:

$$\frac{\dot{\theta}_B(s)}{w_b(s)} = \frac{K_f s^2(\tau_1 s + 1)}{\left(\frac{s^2}{\omega_{n1}^2} + 2\zeta_1 \frac{s}{\omega_{n1}} + 1\right)\left(\frac{s^2}{\omega_{n2}^2} + 2\zeta_2 \frac{s}{\omega_{n2}} + 1\right)} \tag{17}$$

where

$$K_f = 0.766 \times 10^{-2};\ \tau_1 = \frac{1}{8\pi};\ \zeta_1 = \zeta_2 = 0.5$$
$$\omega_{n1} = 2\pi(0.435);\ \omega_{n2} = 2\pi(1.4).$$

These two external inputs were generated numerically [10]. The system parameters used in the simulation are listed in Table I. The sample period T is 0.0025 s, and the control saturation level is ± 10 V.

TABLE I
BRASSBOARD SYSTEM PARAMETERS

ξ_r=0.01	ω_r=2π(166) rad/sec
ξ_g=0.5	ω_g=2π(159) rad/sec
α=−0.16	J=7.34 in-oz-sec^2
K_C=0.1 A/V	K_T=38 in-oz/A
K_G=8.73 V/rad/sec	T_o=4.47 in-oz
Q=250 (in-oz)^2/sec	R_u=1x10^{-7} (rad/sec)^2/V^2

The value for R_u, the weighting parameter in the performance index, was selected by trial and error. As with all

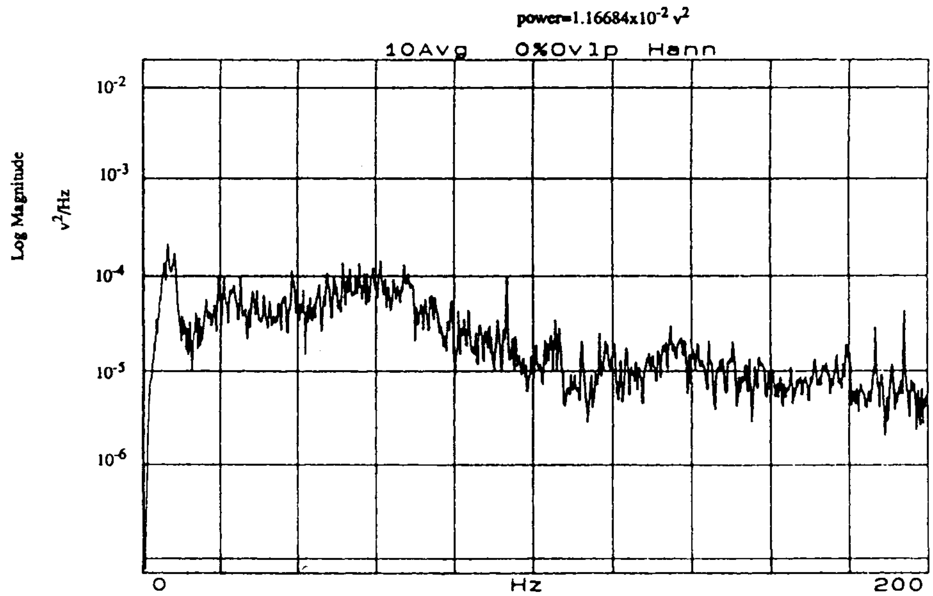

Fig. 9. Power spectral density of error measurement LQG controller.

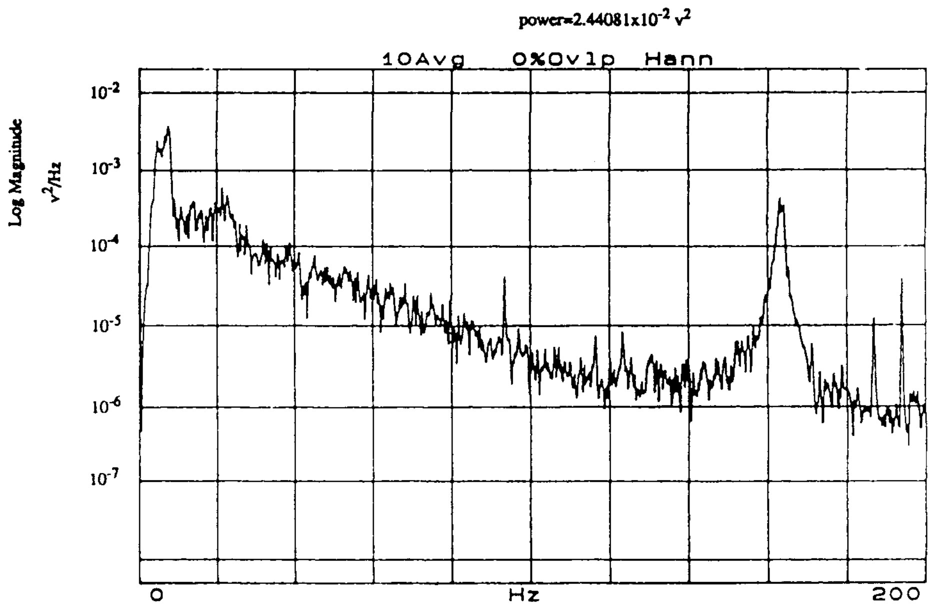

Fig. 10. Power spectral density of measurement z under conventional controller.

LQG formulations, the selection of the performance index weighting parameter represents a simple direct way to fine tune the controller. The sensitivity of the friction estimation algorithm to the value of Q has been investigated extensively [2], [3]; the results indicate very little change in performance for values of Q greater than 200 (in-oz)^2/s.

The time history of $\dot{\theta}$, and the corresponding required control u, are shown in Figs. 3 and 4, respectively. These results correspond to a command rate $\dot{\theta}_c$ of zero. Notice in Fig. 4 that $\dot{\theta}$ remains within a bound of approximately ± 5 mrad/s.

To demonstrate the significance of the control, $\dot{\theta}$ with and without control is shown in Fig. 5. The results reveal an improvement of as much as 40 times for this particular set of parameters. This quality in performance is partially explained by the ability of the estimator to estimate the friction and then the controller to properly compensate for it. As shown in Fig. 6, the estimate of the friction $\hat{T}_f$ very accurately follows the actual simulated friction T_f. It is important to note that the simulated friction actually takes on values between the bounds of $\pm T_0$ due to the fact that a continuous function was used for T_f near the origin for purposes of numerical stability; this is demonstrated in Fig. 7. In order to demonstrate how fast the controller responds to changes in the command input, the response to a step input is shown in Fig. 8.

VI. Brassboard Control Study

In order to evaluate the true potential of this algorithm for modeling and compensating for bearing friction, the estimation and control equations were implemented on a TMS320 microprocessor. Estimates and control values were generated in real time and input to the torque motor on the gimbal to compensate for the bearing friction. The base of the gimbal was excited by a motion generator with a gyro providing rate feedback.

The power spectral density of the angular error θ is shown in Fig. 9. It is of interest to note that the mean square value of the error is 11.67 mV^2 (rms $= 3.42$ mV). The significance of this result is realized by comparing it with the performance of a conventional PI controller with a notch filter. This PI controller and filter was configured and tuned specifically for this brassboard system. This comparison was very important to control engineers at Texas Instruments who have used this type of conventional controller to achieve Type II and Type III forward looking infrared (FLIR) systems for more than 20 years [1]. Examining the power spectral density shown Fig. 10, which corresponds to the conventional controller, the mean square error is observed to be 24.41 mV^2 (rms $= 4.94$ mV). This represents a 44.4% increase in the rms error for the conventional controller as compared to the LQG controller. Power spectral density plots were chosen to present the laboratory results because they so vividly illustrate how the LQG controller effectively compensates at both the low frequencies and at the structural resonance frequency compared to the PI controller with notch filters. Thus, using the LQG algorithm, years of experience at fine tuning controllers and notch filters are not required to achieve effective compensation. The LQG algorithm automatically fine tunes the controller and notch filters based on the assumed system dynamics.

VII. Conclusions

The LQG control algorithm coupled with a Kalman estimator provided a fast responding identifier and compensator for the bearing friction in an inertial stabilization gimbal system. Verification with actual hardware of the ability of the simple exponentially correlated friction model to estimate and compensate for the bearing friction without the need to model stiction and hysteresis effects was achieved. This approach appears to be quite promising for control of gimbal stabilization systems. The improvement in performance over a conventional PI controller with notch filters was quite significant. Since the success of an LQG algorithm is often very dependent on the accuracy of the plant model, a second paper has been written documenting research on a self-tuning algorithm that dramatically increases the robustness of the LQG algorithm discussed in this paper [8].

References

[1] M. K. Masten and J. M. Hilkert, "Electromechanical system configurations for pointing, tracking, and stabilization applications," *SPIE Proc. 389*, pp. 98–106, May 1987.

[2] B. Li, "Identification and compensation for Coulomb friction in stochastic systems," Ph.D. dissertation, Univ. Texas Arlington, Dec. 1994.

[3] D. A. Hullender and B. Li, "Application of advanced control techniques to line-of-sight stabilization systems," Texas Instruments, Inc., Dallas, TX, Final Rep., Feb. 1994.

[4] P. R. Dahl, "Solid friction dampening of mechanical vibrations," *AIAA J.*, vol. 14, no. 12, pp. 1675–1681, Dec. 1976.

[5] D. Schoenwald, U. Ozguner, and R. Graham, "Control of gimbal dynamics via sensitivity models for uncertainty in friction parameters," in *IEEE Conf. Contr. Applicat.*, Dayton, OH, 1992, pp. 52–57.

[6] D. A. Haessig, Jr. and B. Friedland, "On the modeling and simulation of friction," *Trans. ASME J. Dynamic Syst., Measurement, Contr.*, vol. 113, pp. 354–362, Sept. 1991.

[7] B. Maqueira, *Reference Guide On Friction*, Control Systems Technology Center, Defense Systems and Electronics Group, Texas Instruments, Inc., CSTC Memo. 87-022, May 1990.

[8] B. Li and D. A. Hullender, "A self-tuning controller for nonlinear inertial stabilization systems," *IEEE J. Contr. Syst. Technol.*, vol. 6, Mar. 1998.

[9] A. E. Bryson and Y.-C. Ho, *Applied Optimal Control: Optimization, Estimation, and Control.* Waltham, MA: Ginn, 1969.

[10] D. A. Hullender, "Generation of a random time series with a specified spectral density function," in *Proc. 1979 JACC.*